arXiv:1607.07314v1 [quant-ph] 25 Jul 2016

Experimental demonstration of robust entanglement distribution over reciprocal noisy channels assisted by a counter-propagating classical reference light

Rikizo Ikuta,[1] Shota Nozaki,[1] Takashi Yamamoto,[1] Masato Koashi,[2] and Nobuyuki Imoto[1]

[1] *Graduate School of Engineering Science, Osaka University, Toyonaka, Osaka 560-8531, Japan*
[2] *Photon Science Center, The University of Tokyo, Bunkyo-ku, Tokyo 113-8656, Japan*

We experimentally demonstrate a proposal [Phys. Rev. A **87**, 052325 (2013)] of a scheme for robust distribution of polarization entangled photon pairs over collective noisy channels having the reciprocity. Although the scheme employs the robustness of two qubit decoherence-free subspace, by utilizing the forward propagation of one half of the entangled photons and the backward propagation of a classical reference light, it achieves an entanglement-sharing rate proportional to the transmittance of the quantum channel for the signal photon. We experimentally observed the efficient sharing rate while keeping a highly entangled state after the transmission. We also show that the protection method is applicable to transmission of arbitrary polarization state of a single photon.

Faithful and efficient distribution of photonic entangled states through noisy and lossy quantum channels is important for realizing various kinds of quantum information processing, such as quantum key distribution [1–3], quantum repeaters [4], and quantum computation between distant parties [5, 6]. A decoherence-free subspace (DFS) formed by multiple qubits is useful to overcome fluctuations during the transmission which cause disturbance on quantum states. So far, a lot of proposals and demonstrations for faithful transmission of photonic quantum states in a DFS against collective noises have been actively studied [7–16]. However, for DFS protocols formed by two or more photons to succeed, all of the photons must arrive at the receiver side, which seriously limits the distribution efficiency of quantum states. When a two-photon DFS is used for faithful quantum communication over a dephasing channel [12, 17], the transmission rate of the quantum state is proportional to T^2, where T is the transmittance of a single photon. When we consider a random unitary (depolarizing) quantum channel, a four-photon DFS is needed to encode a signal photon state [10, 17, 18], which leads to a transmission rate in the order of T^4.

The inefficiency of such early DFS schemes has been resolved in the case of entangled photon pairs distributed over the dephasing channel [19]. The scaling of the achieved efficiency of sharing entanglement is proportional to T instead of T^2. The key idea to improve the efficiency in the scheme is to prepare a reference single photon for the DFS from a coherent light pulse with average photon number of $\mathcal{O}(T^{-1})$ which backward-propagates in the quantum channel from the receiver to the sender of the signal photon. Recently, an entanglement distribution scheme against general collective noises with an efficiency proportional to T has been proposed [20]. This scheme uses the above idea and another key idea proposed in Ref. [12] which protects quantum states against general collective noises by using the two-photon DFS against the collective dephasing noise at the price of using two communication channels and receiving a constant loss. Such state protection is provided by the reciprocity of the quantum channel and a property of the quantum entanglement that disturbance on one half is equivalent to disturbance on the other half. In this paper, we report an experimental demonstration of the entanglement distribution scheme [20] with an efficiency proportional to T against collective noises including not only the phase noise but also the bit flip noise. We also show that the protection method is applicable to distributing any single photon quantum state with the use of the quantum parity check [21].

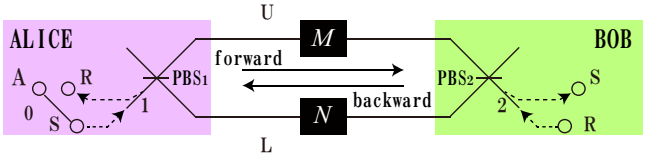

FIG. 1. (Color online) Entanglement distribution protocol by using a counter-propagating photon as a reference light [20]. When photons S and R are reached at port 2 and 1, respectively, the entangled photon pair between Alice and Bob is extracted by the quantum parity check on photons A and R.

We first review the protocol for sharing an entangled photon pair against general collective noises proposed in Ref. [20], in which it is assumed that the party is allowed to use two noisy channels. The conceptual setup of the protocol is shown in Fig. 1. First the sender Alice prepares a maximally entangled photon pair A and S as $|\phi^+\rangle^{\rm AS} \equiv (|{\rm H}\rangle^{\rm A}|{\rm H}\rangle^{\rm S} + |{\rm V}\rangle^{\rm A}|{\rm V}\rangle^{\rm S})/\sqrt{2}$, and sends the signal photon S to Bob after injecting the photon to a polarization beamsplitter ($\rm PBS_1$) connected to two quantum channels from port 1. Here $|{\rm H}\rangle$ and $|{\rm V}\rangle$ represent horizontal (H) and vertical (V) polarization states of a photon, respectively. On the other hand, the receiver Bob prepares a reference photon R in the state $|{\rm D}\rangle^{\rm R} \equiv (|{\rm H}\rangle^{\rm R} + |{\rm V}\rangle^{\rm R})/\sqrt{2}$, and sends it to Alice after injecting the photon to another PBS ($\rm PBS_2$) from port

2.

At the noisy quantum channels, unknown polarization transformations are added on the photons. For the forward (backward) propagation from Alice (Bob) to Bob (Alice), we denote the linear operators of lossy linear optical media for upper (U) and lower (L) optical paths in Fig. 1 by $M_{\rm f(b)}$ and $N_{\rm f(b)}$, respectively. The media satisfy $0 \le M^\dagger_{\rm f(b)} M_{\rm f(b)} \le 1$ and $0 \le N^\dagger_{\rm f(b)} N_{\rm f(b)} \le 1$. As is explained in Ref. [20], for counter-propagating light pulses through any reciprocal media including the situation considered in this paper, Alice and Bob can choose their coordinate systems such that the relationship between the action of the operators on the single photons as

$$\langle i|\Omega_{\rm b}|j\rangle = \langle j|Z\Omega_{\rm f}Z|i\rangle \tag{1}$$

are satisfied for $\Omega = M, N$ and $i, j \in \{{\rm H}, {\rm V}\}$, where $Z = |{\rm H}\rangle\langle{\rm H}| - |{\rm V}\rangle\langle{\rm V}|$. In this paper, we chose the coordinate systems satisfying Eq. (1).

After the transmission through the channels, the separated components of the photons S and R are recombined at $\rm PBS_2$ and $\rm PBS_1$, respectively. Alice and Bob postselect the events of the photon S coming from port 2 and the photon R coming from port 1. As a result, the initial state $|\phi^+\rangle^{\rm AS}|{\rm D}\rangle^{\rm R}$ is transformed as

$$\begin{aligned}|\phi^+\rangle^{\rm AS}|{\rm D}\rangle^{\rm R} \to \quad & (\langle{\rm H}|M_{\rm f}|{\rm H}\rangle\langle{\rm H}|M_{\rm b}|{\rm H}\rangle|{\rm H}\rangle_0^{\rm A}|{\rm H}\rangle_2^{\rm S}|{\rm H}\rangle_1^{\rm R} + \langle{\rm H}|M_{\rm f}|{\rm H}\rangle\langle{\rm V}|N_{\rm b}|{\rm V}\rangle|{\rm H}\rangle_0^{\rm A}|{\rm H}\rangle_2^{\rm S}|{\rm V}\rangle_1^{\rm R} \\ & + \langle{\rm V}|N_{\rm f}|{\rm V}\rangle\langle{\rm H}|M_{\rm b}|{\rm H}\rangle|{\rm V}\rangle_0^{\rm A}|{\rm V}\rangle_2^{\rm S}|{\rm H}\rangle_1^{\rm R} + \langle{\rm V}|N_{\rm f}|{\rm V}\rangle\langle{\rm V}|N_{\rm b}|{\rm V}\rangle|{\rm V}\rangle_0^{\rm A}|{\rm V}\rangle_2^{\rm S}|{\rm V}\rangle_1^{\rm R})/2,\end{aligned} \tag{2}$$

where the subscripts represent the spatial ports of the photons. From Eq. (1), we see that the coefficients of the second and the third terms in Eq. (2) are the same. Thus, by Alice performing the quantum parity check on the photons A and R, whose successful operation is described by $|{\rm H}\rangle_0\langle{\rm H}|_0^{\rm A}\langle{\rm V}|_1^{\rm R} + |{\rm V}\rangle_0\langle{\rm V}|_0^{\rm A}\langle{\rm H}|_1^{\rm R}$, the maximally entangled state $(|{\rm H}\rangle_0|{\rm H}\rangle_2^{\rm S} + |{\rm V}\rangle_0|{\rm V}\rangle_2^{\rm S})/\sqrt{2}$ is extracted. The success probability of the protocol is given by $|\langle{\rm H}|M_{\rm f}|{\rm H}\rangle\langle{\rm V}|N_{\rm f}|{\rm V}\rangle|^2/2$. In our experiment, we construct the lossy and noisy channels by $M_{\rm f(b)} = TU^{\rm u}_{\rm f(b)}$ and $N_{\rm f(b)} = TU^{\rm l}_{\rm f(b)}$, where $U^{\rm u}_{\rm f(b)}$ and $U^{\rm l}_{\rm f(b)}$ are unitary operators, and T is a transmittance of an identical polarization-independent linear loss component. Since the two channels are independent, the success probability becomes $T^2T_{\rm u}T_{\rm l}/2$, where $T_{\rm u}$ and $T_{\rm l}$ are given by average values of $|\langle{\rm H}|{U_{\rm f}}^{\rm u}|{\rm H}\rangle|^2$ about $U^{\rm u}_{\rm f}$ and $|\langle{\rm V}|{U_{\rm f}}^{\rm l}|{\rm V}\rangle|^2$ about $U^{\rm l}_{\rm f}$, respectively. If $U^{\rm u}_{\rm f}$ and $U^{\rm l}_{\rm f}$ are completely random, we obtain $T_{\rm u} = T_{\rm l} = 1/2$. In the experiment, while we switch the unitary operators discretely as described later, the transmission is kept to $T_{\rm u} = T_{\rm l} = 1/2$, resulting in the success probability of $T^2/8$.

The efficiency $\mathcal{O}(T^2)$ of sharing the entangled states is improved by using a weak coherent light pulse (wcp) instead of using the single photon for R. Suppose that average photon number of the wcp received by Alice is μ, which means that Bob prepares the wcp of average photon number μT^{-1}. Since the quantum channel considered in this paper is a linear optical channel, the protocol with the use of the wcp for R works well as was described above when Alice receives one photon in the pulse R and Bob receives the signal photon S, which occurs at a probability of $\mathcal{O}(\mu T)$. Unfortunately, a conventional quantum parity check with linear optics and threshold photon detectors at Alice's side cannot perfectly discard the cases with multiple photons received in the pulse R. Such unwanted events occur at a probability of $\mathcal{O}(\mu^2 T)$ and they degrade the fidelity of the final state. As a result, by choosing the value of μ independent of T such that $1 \gg \mu$ is satisfied, a high-fidelity entangled photon pair is shared because of $\mathcal{O}(\mu T) \gg \mathcal{O}(\mu^2 T)$, with an overall success probability proportional to T as $\mathcal{O}(\mu T)$.

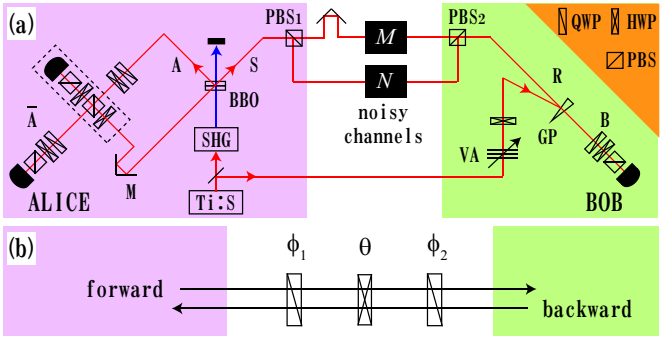

FIG. 2. (Color online) (a) Our experimental setup. The component surrounded by a broken line is the quantum parity check for extracting and decoding the DFS. (b) The reciprocal noisy channel denoted by M or N in Fig. 2 (a). The operation is $Q(\phi_2)H(\theta)Q(\phi_1)$ for the forward-propagating photons, and is $Q(-\phi_1)H(-\theta)Q(-\phi_2)$ for the backward-propagating ones.

The experimental setup is shown in Fig. 2 (a). Light from a mode-locked Ti:sapphire (Ti:S) laser (wavelength: 790 nm; pulse width: 100 fs; repetition rate: 80 MHz) is divided into two beams. One beam is used at Alice's side. It is frequency doubled (wavelength: 395 nm; power: 75 mW) by second harmonic generation (SHG) for preparing $|\phi^+\rangle^{\rm AS}$ through spontaneous parametric down conversion (SPDC) by a pair of type-I and 1.5-mm-thick β-barium borate (BBO) crystals. The photon

pair generation rate is $\gamma \approx 2 \times 10^{-3}$. Photon S enters the two noisy channels after PBS_1. After passing through the noisy channels, the H- and V-polarized components are extracted and recombined by PBS_2, and goes to a photon detector in mode B after an wedged glass plate (GP) whose reflectance is less than 10%. The other beam from the Ti:S laser is used to prepare a wcp as a reference light R at Bob's side. The intensity of the wcp is adjusted by a variable attenuator (VA) in such a way that $\mu \approx 0.9 \times 10^{-1}$ when it arrives at Alice's side after PBS_1. The polarization of the wcp is set to the diagonal polarization by a half wave plate (HWP) after VA. The wcp R is reflected by GP and it propagates the noisy channels after PBS_2 along the same spatial paths as photon S.

After the transmission of photons through the quantum channels, Alice performs the quantum parity check for extracting the DFS and decoding to the qubit state of the single photon, which is shown in the broken box in Fig. 2 (a). After the reference light pulse R passing through the HWP which flips H (V) to V (H), Alice mixes the light pulses A and R at a PBS with a temporal delay adjusted by mirrors (M). Then she projects the photons coming from one of the output ports of the PBS onto the diagonal polarization. Alice postselects the cases where at least one photons are detected at both output modes of the PBS. On the other hand, Bob postselects the cases where at least one photon appears in mode B. Under this post-selection rule, Alice and Bob share the photon pairs in modes $\overline{\mathrm{A}}$ and B which are in state $|\phi^+\rangle_{\overline{\mathrm{A}}\mathrm{B}}$ ideally. All detectors are silicon avalanche photon detectors which are coupled to single-mode optical fibers after spectral filtering with a bandwidth of 2.7 nm.

In this experiment, we simulate a lossy depolarizing quantum channel for each noisy channel. The channel is composed of one HWP sandwiched by two quarter wave plates (QWPs) as shown in Fig. 2 (b). The operations of a HWP and a QWP acting on a single photon are described by $H(\theta) = \cos(2\theta)Z - \sin(2\theta)X$ and $Q(\phi) = (iI - \cos(2\phi)Z + \sin(2\phi)X)/\sqrt{2}$, respectively [22], where $I = |H\rangle\langle H| + |V\rangle\langle V|$, $X = |H\rangle\langle V| + |V\rangle\langle H|$ and $Y = -i|H\rangle\langle V| + i|V\rangle\langle H|$. Here θ and ϕ are rotation angles of the wave plates. The operation $Q(\phi_2)H(\theta)Q(\phi_1)$ on forward-propagating photons works as I, X, Y and Z for the settings of $(\phi_1, \theta, \phi_2) = (0, 0, 0)$, $(0, -\pi/4, 0)$, $(\pi/2, -\pi/4, 0)$ and $(\pi/4, 0, \pi/4)$, respectively, up to global phases. For the backward-propagating photons, the operation of the channel becomes $Q(-\phi_1)H(-\theta)Q(-\phi_2)$. This results in the operation of the backward channel as I, X, Y and Z for the above four angle settings. For simulating the two depolarizing channels, and we slowly switched among the four settings of the wave plates independently in the two noisy channels. When we introduce the photon loss, we insert identical neutral density (ND) filters in the two channels.

We first performed the quantum state tomography [22] of the initial photon pair in modes A and S prepared by the SPDC. We reconstructed the density operator ρ_{AS} of the two-photon state with the use of the iterative maximum likelihood method [23]. The observed fidelity to the maximally entangled state $|\phi^+\rangle_{\mathrm{AS}}$ was 0.97 ± 0.01, which shows Alice prepares a highly entangled photon pair.

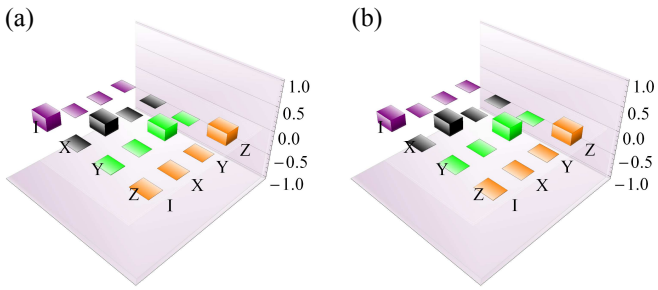

FIG. 3. (Color online) (a) The real part of the reconstructed process matrix for the forward propagation. (b) is one for the backward propagation.

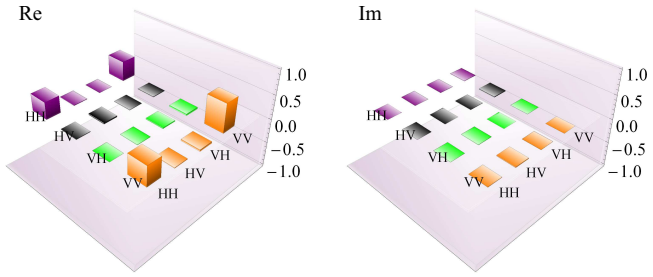

FIG. 4. (Color online) The reconstructed density matrix for $T = 1$.

Before we perform the entanglement distribution by the DFS, we performed the process tomography [24] of the noisy channel composed of the three wave plates for forward and backward propagation of photons. For this, we sent the photon S entangled with photon A to the noisy channel with the forward and backward configuration, and then we performed the state tomography of the two-photon output state. When we sequentially switch the angles of the wave plates for simulating I, X, Y and Z, the process matrices of the channel are reconstructed as shown in Figs. 3 (b) and (c), by assuming that the initial state is the perfect entangled state $|\phi^+\rangle_{\mathrm{AS}}$. We see that the quantum channel well simulates the depolarizing channel for both directions.

Next, we performed our DFS scheme. When we inserted no ND filters to the channels which is regarded as the case of transmittance $T = 1$, the reconstructed density operator of the photon pair shared between Alice

T	Fidelity	Purity	EoF	Fidelity$^{\rm th}$
1	0.89 ± 0.02	0.83 ± 0.03	0.69 ± 0.06	0.85 ± 0.01
0.48	0.85 ± 0.02	0.79 ± 0.03	0.63 ± 0.06	0.83 ± 0.02
0.17	0.87 ± 0.02	0.80 ± 0.04	0.66 ± 0.06	$0.89^{+0.02}_{-0.03}$

TABLE I. The experimental results of the fidelity, purity and entanglement of formation (EoF) of the reconstructed density operators distributed by our scheme for each transmittance T. Fidelity$^{\rm th}$ is the value predicted by the theoretical model with the experimental parameters, in which the error bars come from the observed values of the visibility of the mode matching between the light pulses at Alice's side.

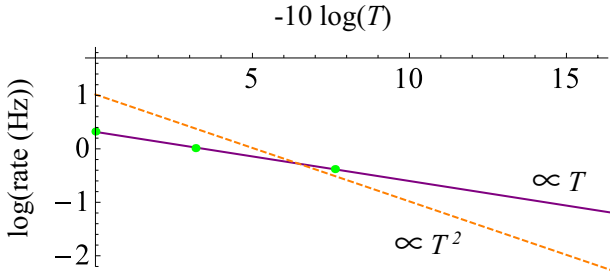

FIG. 5. (Color online) The observed count rate of the states protected by the DFS. The solid line fitted to the experimental data proportional to $T^{0.92\pm0.02}$. The broken line proportional to T^2 is expected when the 2-qubit DFS method with a forward-propagating reference single photon [12] is used. We assumed that the encoding and decoding are performed by using a conventional linear optics [12]. The line passes through a value $\mu^{-1}/2$ times as large as the observed rate for $T = 1$.

and Bob were shown in Fig. 4. The fidelity, the purity and entanglement of formation (EoF) of $\rho_{\rm AB}^{T=1}$ are 0.89 ± 0.02, 0.83 ± 0.03 and 0.69 ± 0.06, respectively. The result shows that the DFS scheme protects the entanglement against collective depolarizing noises. When we inserted ND filters to the channels for T to be ≈ 0.48 and ≈ 0.17, in order for μ to be a constant at Alice's side, we chose the intensity of the reference light pulse R at Bob's side to be T^{-1} times as high as that for the case of $T = 1$. The observed fidelity, the purity and EoF of the reconstructed state for each transmittance are shown in Table I. For all T, the highly entangled photon pairs were shared between Alice and Bob. The sharing rate of the final states for each T is shown in Fig. 5, which shows that the sharing rate is proportional to T. Fidelities predicted by experimental parameters with a theoretical model which deals with multiple photon emission events and mode matching between the photon in mode A and the wcp are shown in Table I, and they are in good agreement with the observed values. In the model, the main causes of the degradation of the entanglement are multiple photons from the photon pair and the coherent light pulse, and mode mismatch at the quantum parity check. The ratios of both errors to the desired events are

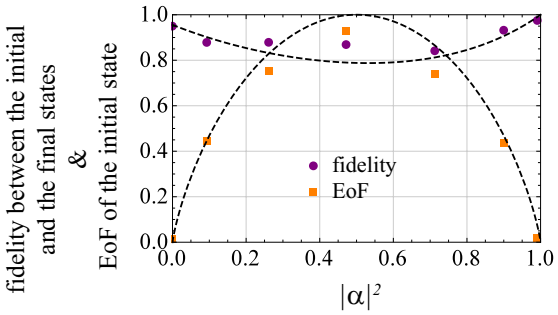

FIG. 6. (Color online) The fidelity between the initial and the final states (circle), and the EoF of the initial state (square) for various values of $|\alpha|^2$ which is estimated from the probabilities of the component $|{\rm HH}\rangle$ of the initial state. A dashed curve for EoF is given by using the ideal state of $|\phi_{\alpha,\beta}\rangle$. A dashed curve for the fidelity is given by the inner product between $|\phi_{\alpha,\beta}\rangle$ and the final state with considering the multiple emission events and the mode matching effect.

almost independent of the transmittance T. As a result, the DFS scheme will work well as long as the count rate is much larger than the dark count rate of the detectors.

The DFS scheme is applicable to the protection of not only the maximally entangled state but also a state in the form of $|\phi_{\alpha,\beta}\rangle = \alpha|{\rm HH}\rangle + \beta|{\rm VV}\rangle$, where α and β are arbitrary complex numbers satisfying $|\alpha|^2 + |\beta|^2 = 1$. To see this, we prepared such non-maximally entangled states by rotating the polarization of the pump light, and then performed the DFS method. We reconstructed the initial and the final states, and calculated the fidelity between the two states. From the experimental result shown in Fig. 6, the fidelity between the initial and the final states is larger than 0.84 for any value of $|\alpha|^2$. As a result, we see that our DFS method is useful for sharing the state $|\phi_{\alpha,\beta}\rangle$. By using the parity check, any state in $\alpha|{\rm H}\rangle + \beta|{\rm V}\rangle$ can be encoded to the form of $|\phi_{\alpha,\beta}\rangle$ without revealing the values of α and β. Decoding can be performed by measuring the photon at Alice's side by $|{\rm D}\rangle$ after the DFS scheme. This means that any single qubit can be sent from Alice to Bob by using the DFS scheme.

We note that the DFS scheme uses two interferometers, one of which is for sending the photons by two quantum channels and the other is for performing the quantum parity check at Alice's side. In the former interferometer, while unknown phase shift between H and V may be added by the fluctuations of the two quantum channels, it is automatically canceled by the DFS. Thus, it is insensitive to the timing mismatch between the photons passing through the two arms. The latter interferometer used for the quantum parity check is also insensitive to the timing mismatch between the photons from the SPDC and the coherent light pulse R because the two-photon interference [25] is used. In fact, the observed FWHM of the visibility against the timing mismatch is ~ 150 μm which

is much longer than the wavelength of the photons. As a result, the DFS method is totally robust against the fluctuations of the optical circuit, and does not need the control with the wavelength-order precision.

In conclusion, we have demonstrated the robust entanglement-sharing scheme over collective noisy channels. By using the counter-propagating reference classical light with an intensity inversely proportional to the transmittance T of the quantum channel, we experimentally achieved the entanglement-sharing rate proportional to T. We also demonstrated that the DFS method is used to distribute any state in $\alpha|\mathrm{HH}\rangle + \beta|\mathrm{VV}\rangle$, which indicates that it is applicable to distributing any unknown single qubit with the redundant encoding by the quantum parity check. The essence of the scheme is the use of the reciprocal property of the channel and the property of the entanglement that a disturbance of one half is equivalent to that of the other half. Since optical fibers are known to be reciprocal media and its fluctuations are slow enough to satisfy the collective assumption, we believe that our efficient DFS method will be useful to distribute entanglement for optical fiber communication over a long distance. In addition, it may open up a new sensor for detecting non-reciprocal property of the noisy channel by measuring the quantity of entanglement.

We thank Hidetoshi Kumagai for helpful discussion. This work was supported by MEXT/JSPS KAKENHI Grant Number JP26286068, JP15H03704, JP16H02214, JP16K17772.

[1] C. H. Bennett and G. Brassard, Proceedings of IEEE International Conference on Computers, Systems, and Signal Processing, Bangalore, India , 175 (1991).
[2] A. K. Ekert, Phys. Rev. Lett. **67**, 661 (1991).
[3] C. H. Bennett, G. Brassard, and N. D. Mermin, Phys. Rev. Lett. **68**, 557 (1992).
[4] N. Sangouard, C. Simon, H. De Riedmatten, and N. Gisin, Reviews of Modern Physics **83**, 33 (2011).
[5] A. Broadbent, J. Fitzsimons, and E. Kashefi, Universal blind quantum computation, in *Foundations of Computer Science, 2009. FOCS'09. 50th Annual IEEE Symposium on*, pp. 517–526, IEEE, 2009.
[6] Y. Takeuchi, K. Fujii, R. Ikuta, T. Yamamoto, and N. Imoto, Phys. Rev. A **93**, 052307 (2016).
[7] P. G. Kwiat, A. J. Berglund, J. B. Altepeter, and A. G. White, Science **290**, 498 (2000).
[8] Z. D. Walton, A. F. Abouraddy, A. V. Sergienko, B. E. A. Saleh, and M. C. Teich, Phys. Rev. Lett. **91**, 087901 (2003).
[9] J.-C. Boileau, D. Gottesman, R. Laflamme, D. Poulin, and R. W. Spekkens, Phys. Rev. Lett. **92**, 017901 (2004).
[10] M. Bourennane *et al.*, Phys. Rev. Lett. **92**, 107901 (2004).
[11] J.-C. Boileau, R. Laflamme, M. Laforest, and C. R. Myers, Phys. Rev. Lett. **93**, 220501 (2004).
[12] T. Yamamoto, J. Shimamura, Ş. K. Özdemir, M. Koashi, and N. Imoto, Phys. Rev. Lett. **95**, 040503 (2005).
[13] T.-Y. Chen *et al.*, Phys. Rev. Lett. **96**, 150504 (2006).
[14] R. Prevedel *et al.*, Phys. Rev. Lett. **99**, 250503 (2007).
[15] T. Yamamoto *et al.*, New Journal of Physics **9**, 191 (2007).
[16] T. Yamamoto, K. Hayashi, Ş. K. Özdemir, M. Koashi, and N. Imoto, Nature Photonics **2**, 488 (2008).
[17] D. A. Lidar and K. B. Whaley, Decoherence-free subspaces and subsystems, in *Irreversible Quantum Dynamics*, pp. 83–120, Springer, 2003.
[18] J. Kempe, D. Bacon, D. A. Lidar, and K. B. Whaley, Phys. Rev. A **63**, 042307 (2001).
[19] R. Ikuta *et al.*, Phys. Rev. Lett. **106**, 110503 (2011).
[20] H. Kumagai, T. Yamamoto, M. Koashi, and N. Imoto, Phys. Rev. A **87**, 052325 (2013).
[21] T. B. Pittman, B. C. Jacobs, and J. D. Franson, Phys. Rev. A **64**, 062311 (2001).
[22] D. F. V. James, P. G. Kwiat, W. J. Munro, and A. G. White, Phys. Rev. A **64**, 052312 (2001).
[23] J. Řeháček, Z. Hradil, E. Knill, and A. I. Lvovsky, Phys. Rev. A **75**, 042108 (2007).
[24] I. L. Chuang and M. A. Nielsen, Journal of Modern Optics **44**, 2455 (1997).
[25] C. Hong, Z. Ou, and L. Mandel, Physical Review Letters **59**, 2044 (1987).